Earthquakes and Structures, *Vol. 16, No. 3 (2019) 265-277*
DOI: https://doi.org/10.12989/eas.2019.16.3.265

Computational evaluation of experimental methodologies of out-of-plane behavior of framed-walls with openings

Filip Anić[1a], Davorin Penava[*1], Lars Abrahamczyk[2] and Vasilis Sarhosis[3]

[1]Faculty of Civil Engineering and Architecture Osijek, Josip Juraj Strossmayer University of Osijek, Osijek 31000, Croatia
[2]Earthquake Damage Analysis Centre (EDAC), Bauhaus-Universität Weimar, Weimar D-99421, Germany
[3]School of Engineering, Newcastle University, Newcastle upon Tyne, NE4 5TG, UK

(Received November 23, 2018, Revised January 14, 2019, Accepted January 15, 2019)

Abstract. Framed masonry wall structures represent a typical high-rise structural system that are also seismically vulnerable. During ground motions, they are excited in both in-plane and out-of-plane terms. The interaction between the frame and the infill during ground motion is a highly investigated phenomenon in the field of seismic engineering. This paper presents a numerical investigation of two distinct static out-of-plane loading methods for framed masonry wall models. The first and most common method is uniformly loaded infill. The load is generally induced by the airbag. The other method is similar to in-plane push-over method, involves loading of the frame directly, not the infill. Consequently, different openings with the same areas and various placements were examined. The numerical model is based on calibrated in-plane bare frame models and on calibrated wall models subjected to OoP bending. Both methods produced widely divergent results in terms of load bearing capabilities, failure modes, damage states etc. Summarily, uniform load on the panel causes more damage to the infill than to the frame; openings do influence structures behavior; three hinged arching action is developed; and greater resistance and deformations are obtained in comparison to the frame loading method. Loading the frame causes the infill to bear significantly greater damage than the infill; infill and openings only influence the behavior after reaching the peak load; infill does not influence initial stiffness; models with opening fail at same inter-storey drift ratio as the bare frame model.

Keywords: computational evaluation; experimental methodologies; out-of-plane behavior; framed-masonry walls; openings

1. Introduction

Many cities are located on seismically active zones that usually contain seismically vulnerable high-rise buildings (Preciado *et al.* 2015). High-rise buildings are generally made from either reinforced concrete (RC) or structural steel frames which are infilled with certain kind of masonry panels. During an earthquake, the ground motion excites the structure and correspondingly, frames interact with the infill walls (Fenerci *et al.* 2016). This interaction has been heavily investigated in the field of seismic engineering. The ground motion excites frames in an arbitrary direction, although its affect can be generalized into three main components: a) In-plane (IP) behavior; b) Out-of-plane (OoP) behavior; c) Biaxial: previous IP damage on OoP behavior (IP+OoP), opposite (OoP+IP) and simultaneous action. The majority of research has been carried out in the field of IP behavior, while less so in the field of OoP behavior, especially when combined with IP loading (Asteris *et al.* 2017, Pasca *et al.* 2017, Onat and Gul 2018).

OoP behavior has been thoroughly investigated by the field of seismic and blast engineering (Lotfi and Zahrai 2018). Ingrained OoP experimental tests are done by fixing the frame and loading the infill wall. These walls are mostly uniformly loaded with airbags (Abrams *et al.* 1998, Hallquist 1998, Akhoundi *et al.* 2016, Di Domenico *et al.* 2016, Furtado *et al.* 2014), and occasionally with point (Preti *et al.* 2014, Hak *et al.* 2014) or line loads (Petrus *et al.* 2015). This approach is certainly a productive method for blast engineering, but also for wind- and soil- (Jäger *et al.* 2015) induced OoP load. During ground motions, frames are excited as well, not fixed. This is well exhibited in real structures as in Fig. 1. In the state-of-the-art article by Furtado *et al.* (2018), they stated that frames do not play a role if they were subjected to pure OoP behavior. However, that is not evident by the dynamical studies by Tu *et al.* (2007), Henderson *et al.* (1994) Nevertheless, due to inertial forces, the infill is exited as well. As shown in dynamical studies by Fowler *et al.* (1994), panels and frames have different natural frequencies even though they move as a single unit. Tests where the loading was set on the frame rather than the infill were conducted by Henderson *et al.* (1994), Flanagan and Bennett (1999) as a previous OoP damage for IP analysis. The relation between the methods of loading the infill and loading the frame is largely unknown.

Loading in the OoP direction, especially when loaded with airbags, was found to produce beneficial arching action as found by McDowell *et al.* (1956). By developing arching action, structures achieve greater load-bearing and

*Corresponding author, Ph.D.
E-mail: davorin.penava@gfos.hr
[a]Ph.D. Student
E-mail: filip.anic@gfos.hr

http://www.techno-press.com/journals/eas&subpage=7
ISSN: 2092-7614 (Print), 2092-7622 (Online)

Fig. 1 OoP inter-storey drift failure, Muisne earthquake (Ecuador) (photographs from EERI org 2018)

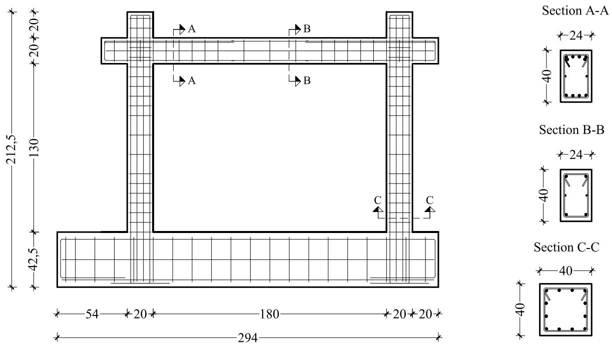

Fig. 2 Reinforcement plan (Penava 2012)

deformation capabilities. Various parameters can limit or even bypass the arching action, such as boundary conditions (Akhoundi *et al.* 2016), openings (Akhoundi *et al.* 2016, Wang 2017, Sepasdar 2017, Dawe and Seah 1989), slenderness of the infill (Moghaddam and Goudarzi 2010), frame stiffness (Dawe and Seah 1989), mortar and masonry characteristics (Abrams *et al.* 1998, Moghaddam *et al.* 2010) and other. Due to arching action, the largest displacements occur near the panels' mid-height.

Canadian provisions (CSA 1978) and those of New Zealand limit calculating OoP capacities via arching action theories (as they do not specify the equation). Others such as those of the MSJC prescribe the use of equation from (Dawe and Seah 1989), while FEMA 356 (2000) prescribes the use of modified Angel *et al.* (1994) equation. Both equations are based on arching action theory. On the other hand, Eurocode 8 provisions EN, BS (2004) limit the slenderness of infill to $h/t<15$. If the slenderness is greater than 15, additional actions for strengthening should be arranged.

In the IP studies, infill walls have considerable effects on the overall behavior, as they change the system's stiffness, failure patterns, loading capacities and etc (El-Dakhakhni *et al.* 2003, Chrysostomou and Asteris 2012, Asteris and Cotsovos 2012b). Furthermore, various macro- and analytical models were developed for the IP analysis (Crisafulli 2000). Conjointly, the inclusion of openings was soughed and implemented in the IP macro-models (Asteris *et al.* 2012a). Contrariwise, in the field of pure OoP (Al Hanoun *et al.* 2019, Ricci *et al.* 2018) and IP+OoP (Di Trapani *et al.* 2018) loading the macro-models are at its infancy. They are based on struts with masses at the middle, and they account only for the inertial methods without the incursion of openings. Similarly, all OoP analytical models of framed masonry (Angel *et al.* 1994, Dawe and Seah 1989, Moghaddam and Goudarzi 2010, Klingner *et al.* 1996) are based on inertial methods. Overall, there are no macro- nor analytical models developed on the basis of inter-storey drift methods.

Consequently, this paper presents a numerical investigation into OoP behavior of a one-storey, one-bay RC frame with an unreinforced masonry infill (URM) wall loaded with both uniform load on the infill and point loads on the frame. The use of RC frames with URM infill is a common practice in seismically active South Europe (Booth and Key 2006). The study is conducted using Atena3D software (Cervenka Consulting 2015). Frames and URM's geometrical and material properties are obtained from Sigmund and Penava (2014), Anić *et al.* (2018a). The aim of this paper is to compare the two approaches and observe the influence of openings.

This paper also considers various types of openings, as their influence on OoP behavior is yet to be investigated systematically. The present studies on openings show opposing results. On the one hand, in the studies by Akhoundi *et al.* (2016), Dawe and Seah (1989), openings did not result in lowering the ultimate force. However, the deformation capabilities were significantly lowered. On the other hand, in the studies by Wang (2017), Sepasdar (2017), a reduction in ultimate force and deformation was observed for both window and door openings. This was also observed in URM wall experiments, as in Griffith *et al.* (2007), and RC walls test by Mays *et al.* (1999). Mays *et al.* (1999) also provides a formula for the linear reduction of ultimate force based on the size of the opening, however; his observation was based on RC walls not framed masonry.

Similar research was performed by Flanagan (1994), where he studied both the inter-storey drift and the inertial method. However, when comparing the approach described in this paper and that of Flanagan (1994), the following differences with have been outlined: a steel frame was used instead of a RC frame; the infill wall did not contain any opening, and the axial force in the columns was not taken into the account.

2. Materials and methods

The geometry of the RC frame originates from a prototype structure which represents a common 7-storey reinforced concrete office building located in the area of high seismicity, designed in compliance with EN1992: EN1998:2004 provisions, as described in detail in Penava (2012), Sigmund & Penava (2014), Zovkić *et al.* (2013). It represents a middle ground storey bay from the middle frame in *x*-direction of the prototype structure. The adopted one-storey one-bay reinforced concrete frame was constructed in a 1/2.5 scale.

RC frames were classified by EN 1992-1-1 (EN, BS 2

(a) Load parallel to headjoints

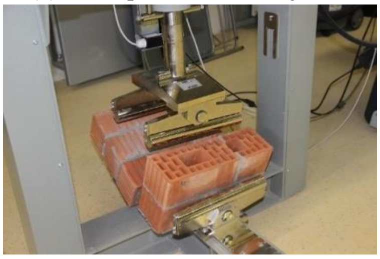

(b) Load parallel to bedjoints

Fig. 3 Wall specimens tested on OoP bending

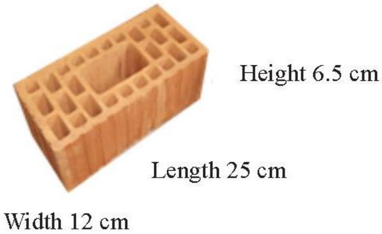

Fig. 4 Clay masonry block used as infill units

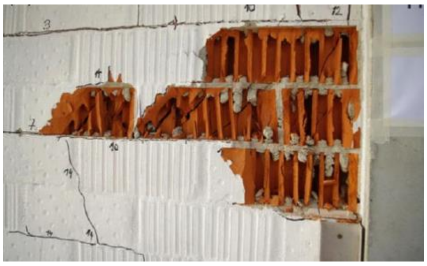

Fig. 5 Interlock effect in real structure (Penava 2012)

2004) and EN 1998-1-1 (EN, BS 2004) provisions as medium ductility class (DCM) frames. Hollow clay masonry blocks, which were used as infill units (Fig. 4), are classified as Group II by the EN 1996-1-1 (EN, BS 2005) provisions. General purpose mortar was used and is classified as M5 by EN 1996-1-1 (EN, BS 2005) provisions.

Table 1 presents the specimens used for the numerical analysis. Originally, they were tested for cyclic quasi-static IP tests by Penava (2012). The opening area (A_o) was selected as 2.0 m^2, which falls within the range A_o>1:5 m^2 and A_o>2:5 m^2 defined by EN 1998-1 (EN, BS 2004). Hence, the opening size does not vary, but its position and proportions do.

In order to investigate differences and similarities between two approaches, the problem was separated into:

Approach 1: OoP load is transmitted onto the infill with uniform load (airbag - inertial method);

Approach 2: OoP load is transmitted onto the frame (inter storey drift method).

The test setup originates from the study described in Penava (2012), Sigmund and Penava (2014), where the model structure was tested under constant normal force of 365 kN applied at the column tops and cyclic IP shear forces applied at the beam ends. In this study; however, only the OoP action was considered, whether by point-load applied to the frame or by uniform load applied to the masonry infill wall. The IP shear forces where not considered, but the rest of test setup was kept the same.

Boundary conditions for Approach 1 were set to mimic the conditions such as in Dawe and Seah (1989), Akhoundi *et al.* (2015), Furtado *et al.* (2015). In those studies, the translation of the beam was fixed, while airbag transmitted uniform area load on the infill. In the case of openings, as in Dawe and Seah (1989), Sepasdar (2017), Akhoundi *et al.* (2016), Wang (2017), plywood was used to cover the opening. However, in this paper openings were neither covered nor loaded; thus, providing more realistic conditions. In Approach 2, the force was applied to the frame beam-column joints only. Same was applied in studies by Flanagan and Bennett (1999), contrary to the approach described in Henderson *et al.* (1994), where the point-load was additionally applied at the half of the columns height. It was considered in this study that the point-loads originate dominantly from the storey inertia forces, therefore the other point-load was not considered.

The self-weight of the masonry infill walls and of the RC slabs was taken into account in the design of the model structure; however, their corresponding part in the model structure (above the RC frame beam) was considered having little impact in this study and in the reference study described in Penava (2012), Sigmund and Penava (2014), Zovkić *et al.* (2013). The realistic response (deformed shape) of the model structure was ensured by supports at column tops, by preventing of vertical displacements and rotation while allowing horizontal sliding. Moreover, in the literature of OoP behavior; most commonly, the gravity force was applied on to the column ends (Abrams *et al.* 1998, Di Domenico *et al.* 2016). Hence, in order to compare the most common loading approaches, the axial loading of columns was used.

2.1 Materials

Infill's mechanical properties are presented in Table 2 and the properties of RC are presented in Table 3. Due to presence of voids in the block, material orthogonality was pronounced, and stronger response is obtained in direction of voids then perpendicularly.

Additional OoP bending tests were carried out in accordance with EN 1052-2 (BSI 2016) provisions. Tests were initiated in order to obtain the infill's OoP behavior characteristics. The results are presented in Anić *et al.* (2018a); in short, it was found that, when the line of the load is parallel with the bedjoints, the wall fails by separating blocks, i.e., due to reaching tensile strength of the mortar. When the line load is perpendicular to the bedjoints, the wall fails by cracking through the block.

The CC Nonlinear Cementitious material model

Table 1 Specimens considered

Model mark	Appearance of the specimen	Opening	
		Type and area	Position
CD	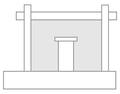	Door l_o / h_o = 0.35 / 0.90 m A_o = 0.32 m^2 A_o / A_i = 0.14	Centric e_o = l_i / 2 = 0.90 m
CW	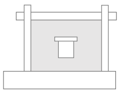	Window l_o / h_o = 50.0 / 60.0 cm A_o = 0.30 m^2 A_o / A_i = 0.13	Centric e_o = l_i / 2 = 0.90 m P = 0.40 m
ED	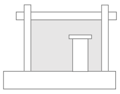	Door l_o / h_o = 0.35 / 0.90 m A_o = 0.32 m^2 A_o / A_i = 0.14	Eccentric e_o = h_i / 5 + l_o / 2 = 0.44 m
EW	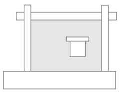	Window l_o / h_o = 50.0 / 60.0 cm A_o = 0.30 m^2 A_o / A_i = 0.13	Eccentric e_o = h_i / 5 + l_o / 2 = 0.44 m P = 0.40 m
BF	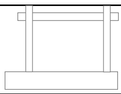	Bare frame	
FI	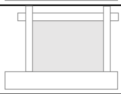	Full infill	

Table 2 Masonry properties obtained by tests

Specimen	Properties		Value	Unit
Clay block (Penava 2012)	Compressive strength ∥ voids	f_b	15.90	MPa
	Compressive strength ⊥ voids	f_{bh}	2.60	MPa
Mortar (Penava 2012)	Mortars compressive strength	f_m	5.15	MPa
	Mortars flexural strength	f_{mt}	1.27	MPa
Wall specimen (Penava 2012)	Characteristic compressive strength	f_k	2.70	MPa
	Elastic modulus	E	3900.00	MPa
	Ultimate strain	ε_u	0.58	‰
	Initial shear strength	f_{vk0}	0.35	MPa
	Friction coefficient	tgα_k	0.24	-
Wall specimens OoP	Flexural strength ∥ to bedjoints	f_x	0.21	MPa
	Flexural strength ∥ to headjoints	f_{xh}	0.36	MPa

Table 3 RC properties obtained by tests Penava (2012)

Entity	Properties		Value	Unit
Concrete	Compressive strength	f_c	58	MPa
Rebar	Yield stress	f_y	550	MPa
	Tension strength	f_t	650	MPa
	Elasticity modulus	E	197430	MPa

Table 4 CC Nonlinear Cementitious 2 material model

Description		Frame concrete	Concrete lintel	Clay block	Unit
Elastic modulus	E	4.100 E+04	3.032 E+04	5.650 E+03	MPa
Poisson's ratio	μ	0.200	0.200	0.100	/
Tensile strength	f_t	4.000	2.317	0.380	MPa
Compressive strength	f_c	-5.800E+01	-2.550E+01	-1.750 E+01	MPa
Specific fracture energy Eq. (3)	G_f	1.200 E-04	5.739 E-05	4.500 E-04	MN/m
Crack spacing	s_{max}	0.125	0.125	/	m
Tensile stiffening	c_{ts}	0.400	0.400	/	/
Critical compressive disp.	W_d	-5.000 E-04	-5.000 E-04	-5.000 E-04	/
Plastic strain at f_c	ε_{cp}	-1.417 E-03	-8.411 E-04	-1.358 E-03	/
Reduction of f_c due to cracks	$r_{c.lim}$	0.800	0.800	0.800	/
Crack shear stiffness factor	S_F	2.000 E+01	2.000 E+01	2.000 E+01	/
Aggregate size		1.600 E-02	2.000 E-02	/	m
Fixed crack model coefficient		1.000	1.000	1.000	/

(Cervenka *et al.* 2012) was used to numerically describe the behavior of the clay block and concrete. The input values are shown in Table 4. It is to be noted that all values, except for tensile strength for the case of clay block in Table 4 represent values tested in the direction of voids. A tensile strength perpendicular to the voids was introduced in order to facilitate reliable OoP bending simulation (Anić *et al.* 2018a).

The interface material model (Cervenka *et al.* 2012), meaning the contact between solid elements, is presented in Table 5. An interlocking effect (Fig. 5) occurs as mortar is laid on the blocks, while mortar slips into the voids and in turn locks two opposite blocks in simultaneous action. The interlocking effect was introduced to the interface material model by interlocking functions (Fig. 6).

In the case of reinforcements, a bilinear steel material model (Cervenka *et al.* 2012) was used, its values are shown in Table 6. Perfect connection between rebar and concrete was used.

$$K_{nn} = E / t \tag{1}$$

$$K_{tt} = G / t \tag{2}$$

Table 5 Interface material properties

Description			Mortar bedjoint Value		Mortar headjoint Value		Unit
Normal stiffness	K_{nn}	Eq. (1)	5.65	E+05	8.50	E+04	MPa
Tangential	K_{tt}	Eq. (2)	2.57	E+05	3.86	E+04	MPa
Tensile strength	f_t		0.20		0.20		MPa
Cohesion	c		0.35		0.35		MPa
Friction	tgα		0.24		0.24		/
Interlocking	Interlocking		see fig.6		/		

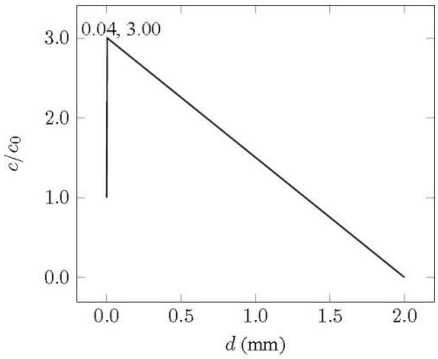

(a) Interlocking function

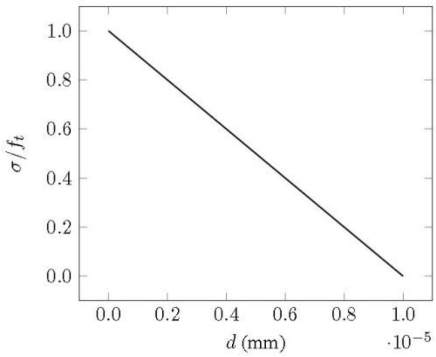

(b) Tension softening

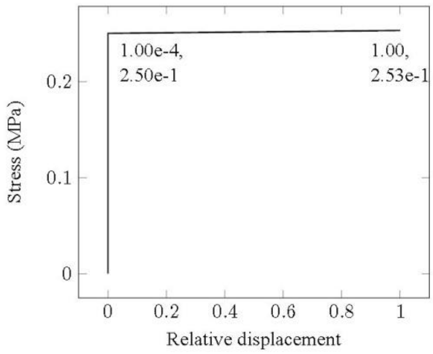

(c) Nonlinear spring

Fig. 6 Functions used for calculation purposes

Where t is mortar thickness (standard thickness of 10 mm).

$$G_f = 0.000025 f_t \tag{3}$$

As the frame represents a part of a bigger structure, a gravity load of 365 kN was introduced to the column ends. Such a normal force produces noticeable friction force T_F and cannot be undermined as is the case during IP simulations of the same model (Anić *et al.* 2017). The friction coefficient of sliding steel rollers, similar to the ones used in the IP test (μ_F), was taken as 0.03 (Hirt & Lebet 2013). Hence, the friction force for one column end was calculated using Eq. (4).

Table 6 Bilinear steel reinforcement properties

Description	Symbol	Value		Unit
Elastic modulus	E	2.10	E+05	MPa
Yield strength	σ_y	5.50	E+02	MPa
Tensile strength	σ_t	6.50	E+02	MPa
Limited ductility of steel	ε_{lim}	0.01		/

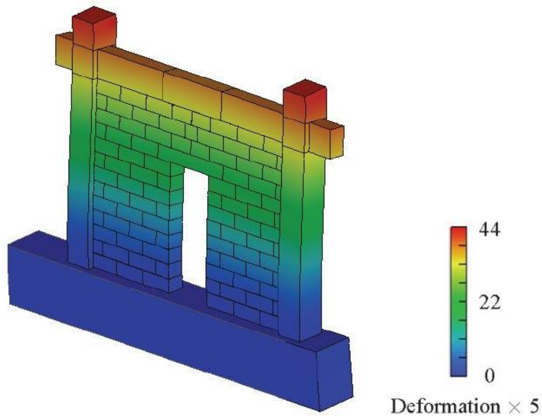

Fig. 7 Displacements in mm of CD model at maximum drift ratio dr

$$T_F = 365 \mu_F \approx 10 \text{ kN} \tag{4}$$

For introducing friction force in to the numerical model, a non-linear surface spring was set on the columns. Spring stiffness was calculated by Eq. (5).

$$K_s = T_F / A_{col} = 0.25 \text{ MPa} \tag{5}$$

The friction spring function is presented in Fig. 6(c). As the normal force is introduced, friction occurs immediately; hence, in this case a small relative displacement was introduced before reaching full stress. A small incline was presented, ranging from 0.250 to 0.253 MPa in order to ensure greater numerical stability.

2.2 Numerical model setup

The numerical model of RC frame (BF model) is based on the calibrated IP cyclic quasi- static model Anić *et al.* 2018b). Hence, the BF can be considered calibrated in the OoP direction as well. The OoP characteristics of the infill were calibrated on bending tests (Fig. 3). The micromodel managed to mimic the failures and ultimate forces as in the experiments. For further reads, please remark the reference Anić *et al.* (2018a).

Numerical models have the same setup up to the point of loading and supports. The characteristics which were identical for both approaches are shown in Fig. 8. Reinforcements were modelled as 1D truss bars. Rebar overlapping was modelled by cumulating rebar areas and applying it to a single bar. Contacts between blocks and those between blocks and frame were modelled as gapped

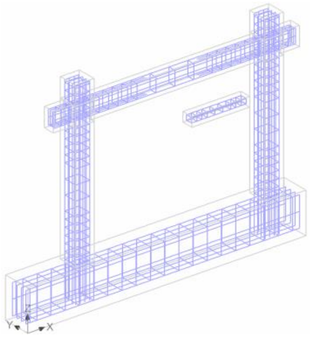

(a) Reinforcement 1D bar

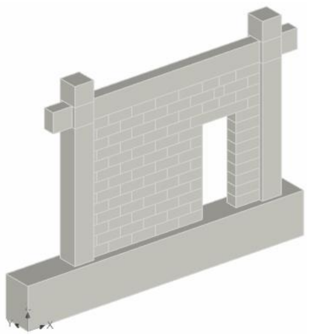

(b) Solid 3D macro elements

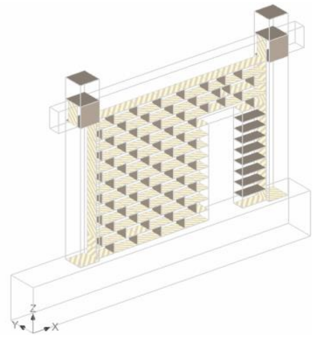

(c) Contacts 2D interface

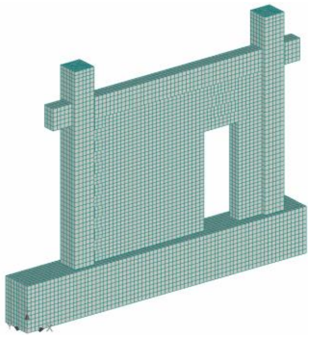

(d) FE mesh

Fig. 8 General model setup on the ED model example

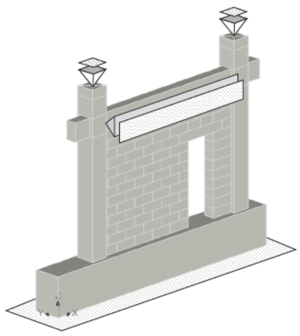

(a) Supports for Approach 1

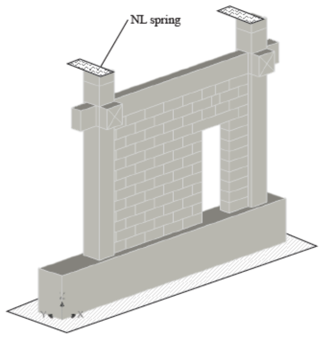

(b) Supports for Approach 2

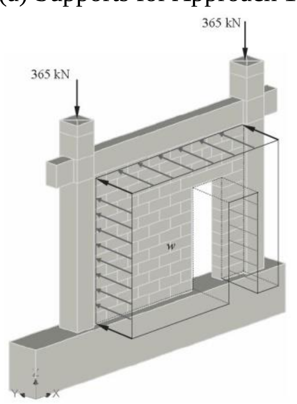

(c) Loading for Approach 1

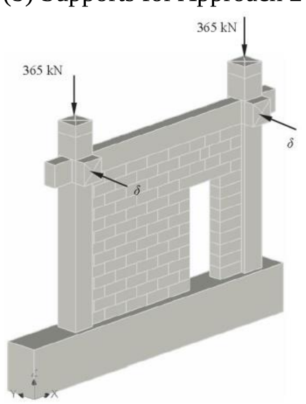

(d) Loading for Approach 2

Fig. 9 Boundary conditions on the ED model example

zero thickness (2D) interfaces, and others with perfect contact. The contact between the frame and infill contained no interlocking functions as the interlocking effect cannot be developed on those areas. Brick mesh with a size of 4 cm was applied to all elements. Few plate elements have mesh

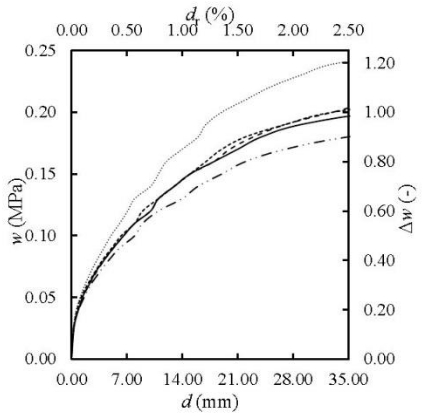

(a) Pressure vs. displacement – Approach 1

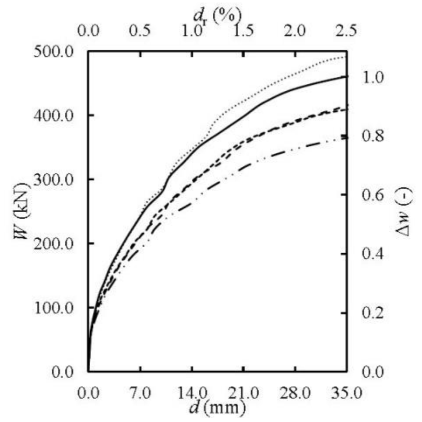

(b) Force vs. displacement – Approach 1

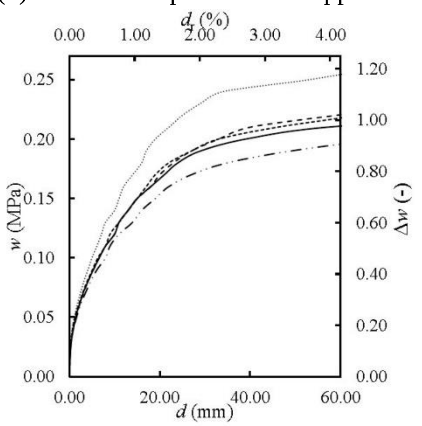

(c) Pressure vs. displacement – Approach 1

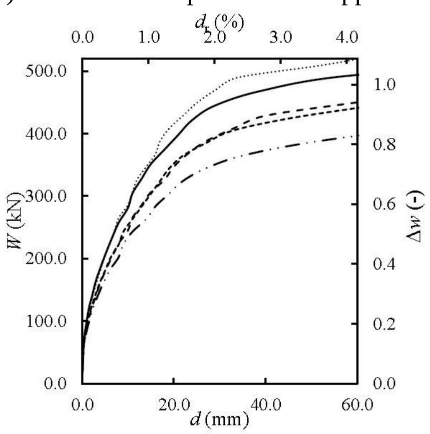

(d) Force vs. displacement – Approach 1

Fig. 10 Load vs. displacement

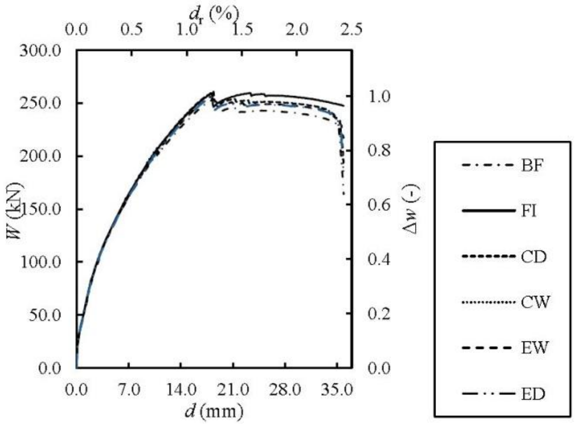

(e) Force vs. displacement – Approach 2

Fig. 10 Continued

with triangulated surfaces due to their geometrical irregularity.

Fig. 9 presents the boundary conditions, where it can be seen that both approaches involve foundation supports fixed in all direction. Both approaches include a vertical force of 365 kN, applied in five steps with 73 kN increments. In the case of Approach 1, the column support in the z direction and beam supports in the y direction are active as soon as the column force was applied. When the column supports were activated, the area load was set on the infill with w=0.002 MPa per step. On the other hand, in the case of Approach 2, after the vertical force was loaded, only column supports in z direction were active, together with the non-linear springs in the y direction to mimic the friction of the rollers. When the column supports were active, the prescribed deformation was activated with a deflection of δ=0.1 mm per step. The model was pushed until it reached a 2.5% drift ratio (d_r).

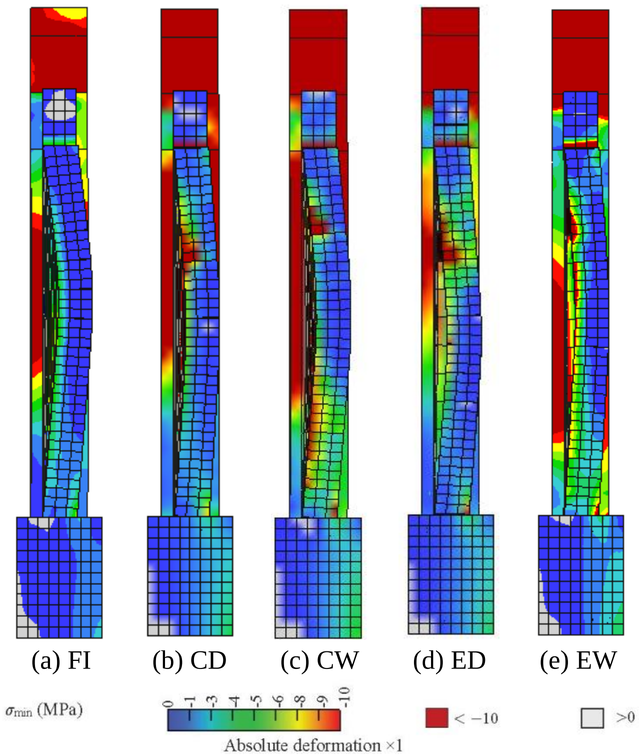

(a) FI (b) CD (c) CW (d) ED (e) EW

Fig. 11 Load vs. displacement

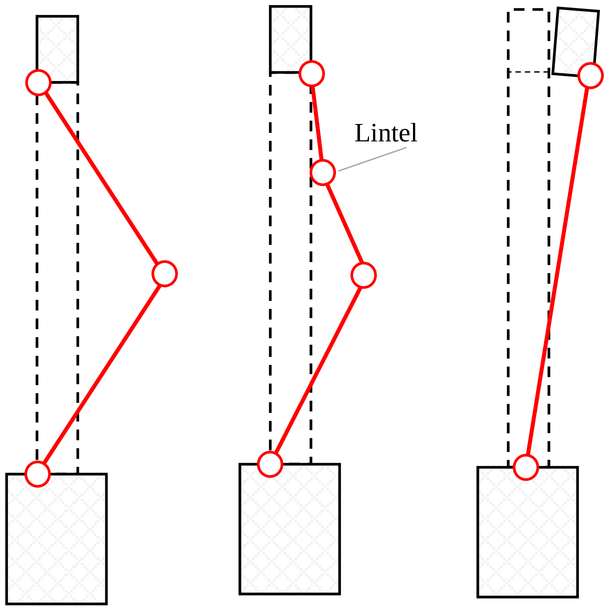

(a) Three-hinged action (b) Four-hinged action (c) Two-hinged action

Fig. 12 Arching actions as observed in Approaches 1 and 2

3. Computations and results

In Fig. 10, a loading versus displacement diagram is shown with displacements and loadings plotted on the primary horizontal and vertical axis. On the secondary vertical axis, load differences (Δw & ΔW) are presented. The referenced value, i.e., Δw & ΔW=1 was set for the maximal force of the FI model. On the secondary horizontal axis, inter-storey drift ratios were plotted (dr). For Approach 1 (Figs. 10(a)-(d)), displacements were measure as global maxima of the panel in y direction. Figs. 10(a), (b) and (e) are plotted to 2.5 % d_r, and Figs. 10(c) and (d), drift ratio was widen to 4% d_r in order to observe the yielding line. In the case of Approach 2, (Fig.10(c)), displacements were measured at point of load input, i.e., column - beam joint. On Fig. 10(a), area pressure w is shown, and in Fig. 10(b) force W calculated using Eq. (6). The force W from Fig. 10(c) represents the sum of forces from each column.

$$W = w\left(A_{\text{infill}} - A_{\text{opening}}\right) \tag{5}$$

In Figs. 13-17, the back surface refers to the side to which the load was applied, and vice versa for the front view. In Fig. 11, minimum principal stresses are plotted on the cross section of the models in Approach 1. The section plane was positioned at the infill's mid-length in the case of the FI model and right beside the opening for the models with openings. In Fig. 12, crack patterns are shown for Approach 1. Similarly, in Fig. 15, crack patterns for Approach 2 are displayed. In Fig. 14, minimal principal stresses at the maximum drift ratio of Approach 1 are shown. Similarly, in Fig. 16, minimal principal stresses of

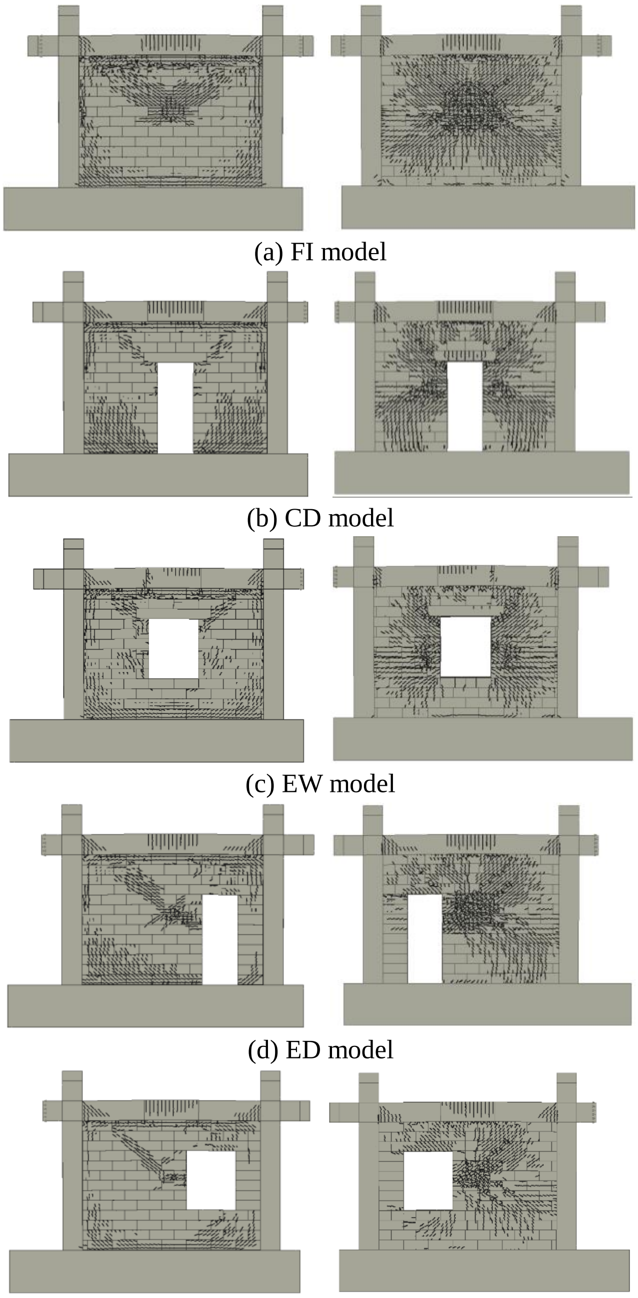

(a) FI model

(b) CD model

(c) EW model

(d) ED model

(e) EW model

Minimum crack width = 0.1 mm ; deformation × 1 ; crack width multiplier ×1

Fig. 13 Approach 1: Crack patterns (left front, right back view)

the frame are shown, while, in Fig. 17, minimal principal stresses of the infill are shown. Both the latter two figures represent the stress under ultimate force. In Fig. 7, displacements in the *y* direction are displayed for the CD model example.

4. Discussion of results

From Fig. 10(b), it is clear that, in Approach 1, openings, in terms of their composition and placement do effect OoP behavior. This was also found in the work by Wang (2017), Sepasdar (2017). On the other hand, from Figure 10c, it is noticeable that, with Approach 2, the influence of openings is negligible in terms of forces and displacements before the peak load. In studies by Akhoundi *et al.* (2016), Flanagan and Bennett (1999) openings did not influence initial stiffness nor the ultimate force. The differences are noticeable after reaching the peak load. In detail, after reaching the peak load, models with openings do not defer from each other, while they obtain slightly greater forces in comparison to BF and slightly lower loads when compared to the FI model. Moreover, models with openings fail at the same drift ratio as the BF model. The FI model showed more prominent behavior after reaching peak load, as it did not fail, as well as acquired better post-peak load-bearing behavior. With Approach 2, it is noticeable that the infill did not influence the initial stiffness of the frame, although it did influence post-peak stiffness (Fig. 10(d)). The infill’s negligible influence on the initial stiffness of the frames can be observed in the findings of dynamic studies conducted on bare and infilled frames by Tu *et al.* (2007).

The CW model almost had an identical load - deflection response as the FI model with the Approach 1 (Figs. 10(b), 10(d)). The same pre-ultimate load - deflection response was found between the centric window and the full frame specimen in studies by Akhoundi *et al.* (2016). Hence, when compared to the CD model, it is noticeable that size composition does influence the response.

Furthermore, comparing EW to CW and ED to CD, model, one can observe that, in the case of Approach 1, the location of opening does influence the outcome (Figs. 10(b), 10(d)).

From Fig. 7, it is noticeable that displacements obtained from Approach 2 range from zero at the foundation to the maximum at the column’s end. This is consistent with findings in the OoP studies on the shaking table test by Tu *et al.* (2007). In Fowler *et al.* (1994), maximal accelerations were observed at top of the panel. Furthermore, displacements of the infill and the frame are identical. Hence, the frame and the infill behave as a single element. The same was observed in dynamical tests by Fowler *et al.* (1994), where relative and absolute displacements between the frame and the infill were almost zero.

Torsion of the beam can be observed in Fig. 7. The combination of torsion and translation of the beam can cause infill to lose the upper row, as observed in the infill of a three-storey building excited in the OoP direction by a shaking table (Penava *et al.* 2018). The effects of beam torsion were as well observed and implemented in the calculation of OoP capacity by Dawe and Seah (1989).

By examining Figs. 11 and 16, it is clear that a compression arch has developed for both models with and without openings. The FI model in Fig. 11(a) displays three supports where infill clamps at the panel’s mid height and at the beams. Those three points form a three-hinged arching action (Fig. 12(a)), which is common for two- and one-way arching action. In the case of openings, there is an accumulation of stress in the lintel (Figs. 11(b)-(e) and 16(b)-(e)), hence an additional support is formed. This means that one can assume that a four-hinged action (Fig. 12(b)) forms with an additional point at the lintel. This

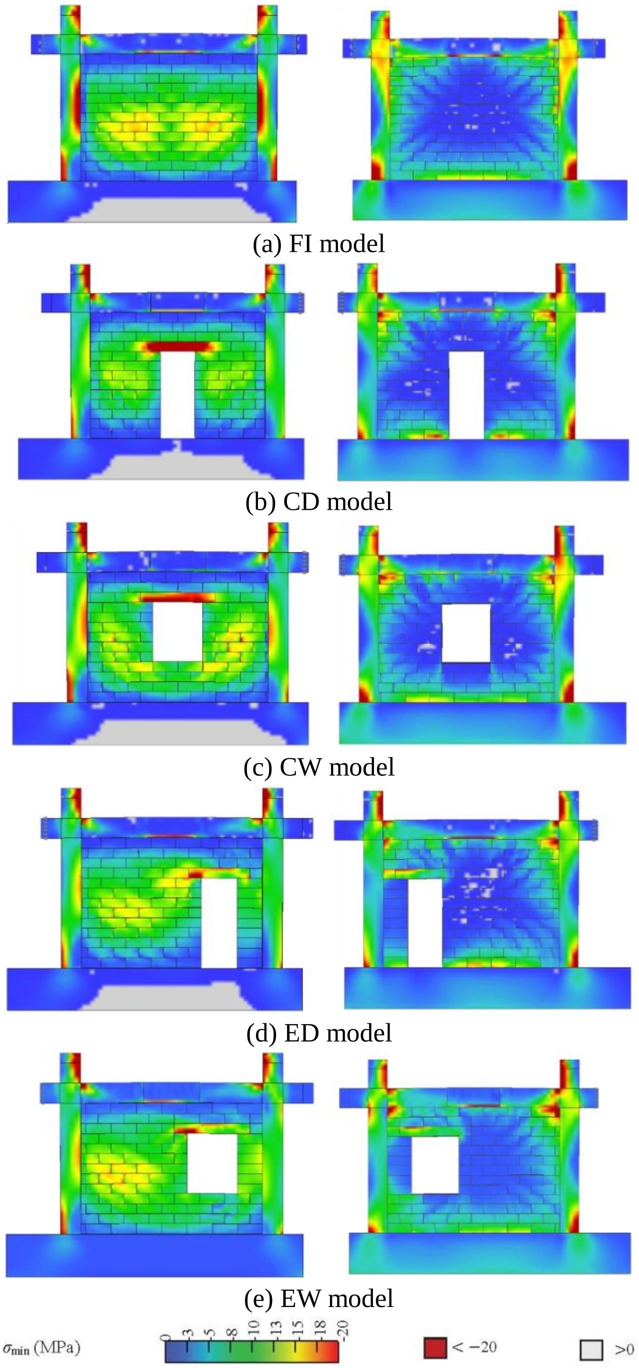

Fig. 14 Approach 1: Minimum principal stress (left front, right back view)

additional hinge, along with the reduced area of the panel may cause a reduction in deformation capabilities as observed by Akhoundi *et al.* (2016).

Regarding the stress distribution for Approach 2 (Fig. 17), the ingrained arching action was not obvious. Rather, the two-hinged arching action (Fig. 12) occurred. That said, the arch did not form but a compression thrust did. However, for the sake of consistency, it will be regarded as an arch. The prominent position of the two-hinged action is found near the columns, due to the same displacements on relation column - infill. The two-hinged action was also observed in the shaking table test by Tu *et al.* (2007).

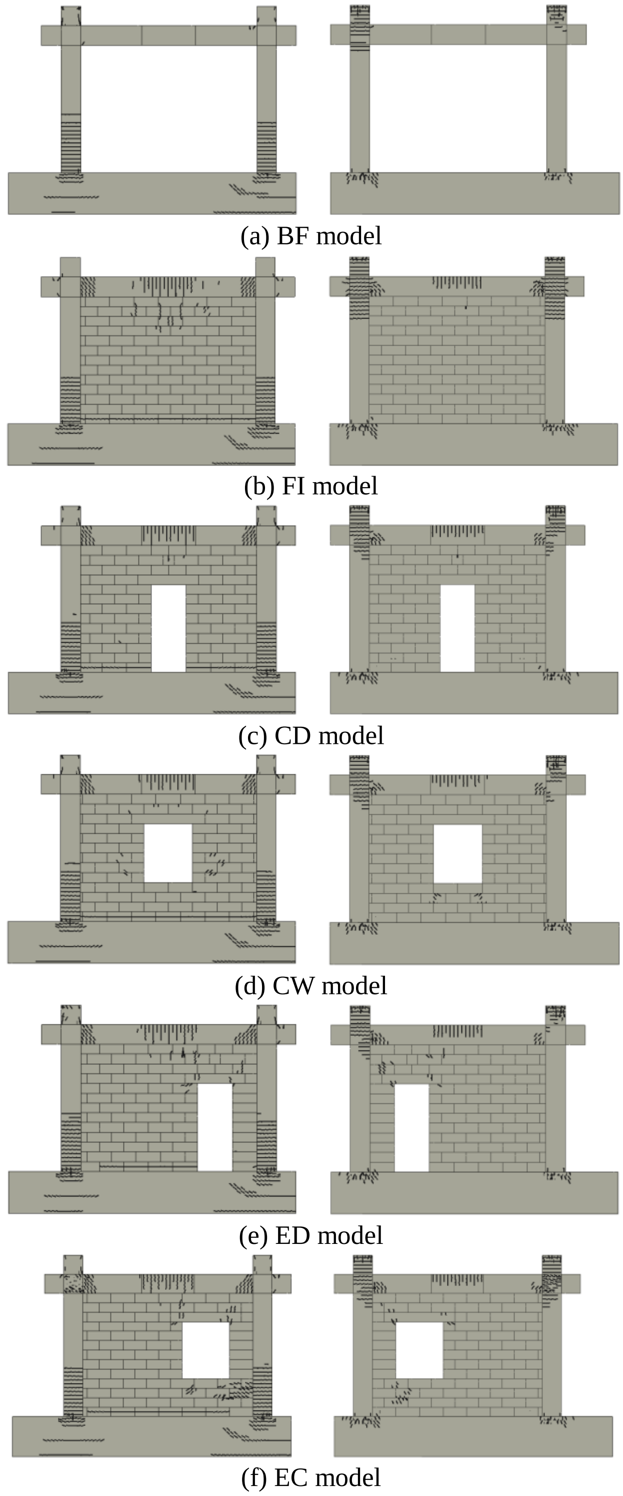

Min. crack width = 0.01 mm, Shift cracks outwards ×1,
Crack width multiplier × 1, Deformation ×1

Fig. 15 Approach 2: Crack patterns maximum drift ratio d_r (left front, right back view)

When comparing minimum principal stresses between the frame and infill, it is noticeable that, in the case of Approach 1, these obtained stress within the same range (Fig. 14). This resulted in heavy damage to the infill and slight damage to the frame. However, in the case of Approach 2, stress differed as much as 10 times between

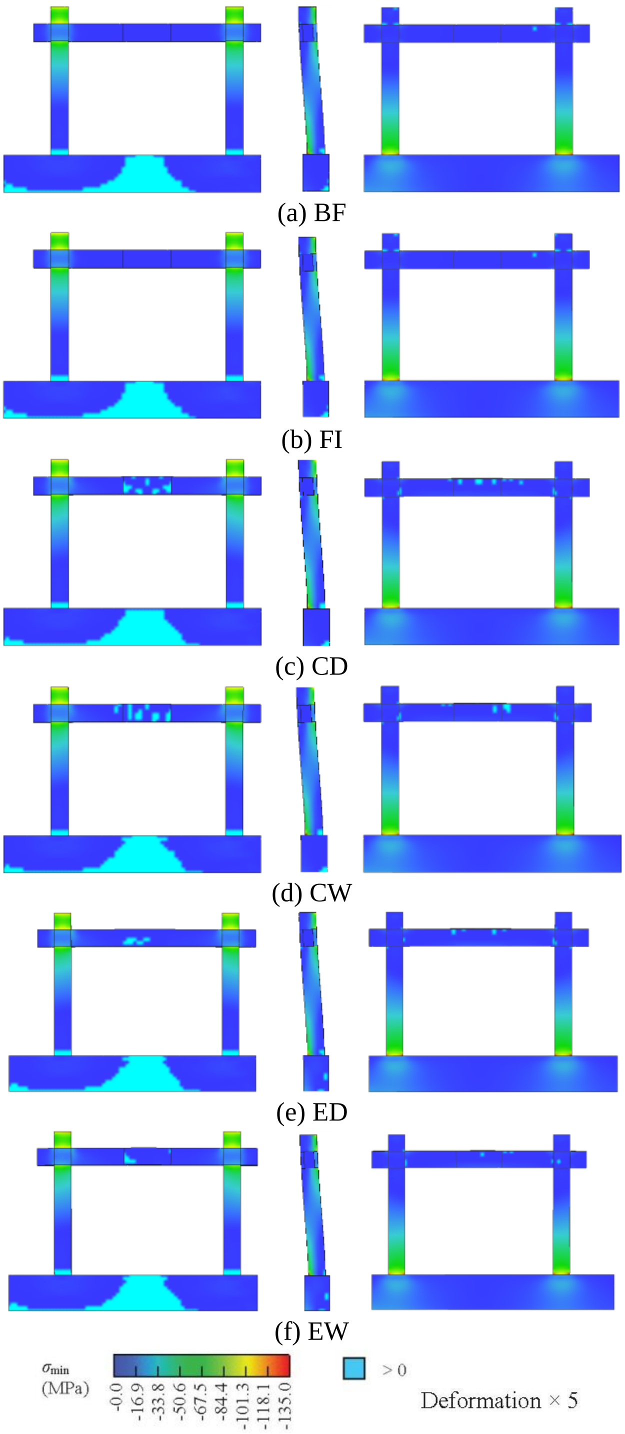

Fig. 16 Approach 2: Minimum principal stress of the frame at maximum force *W* (left front, rig-th back view)

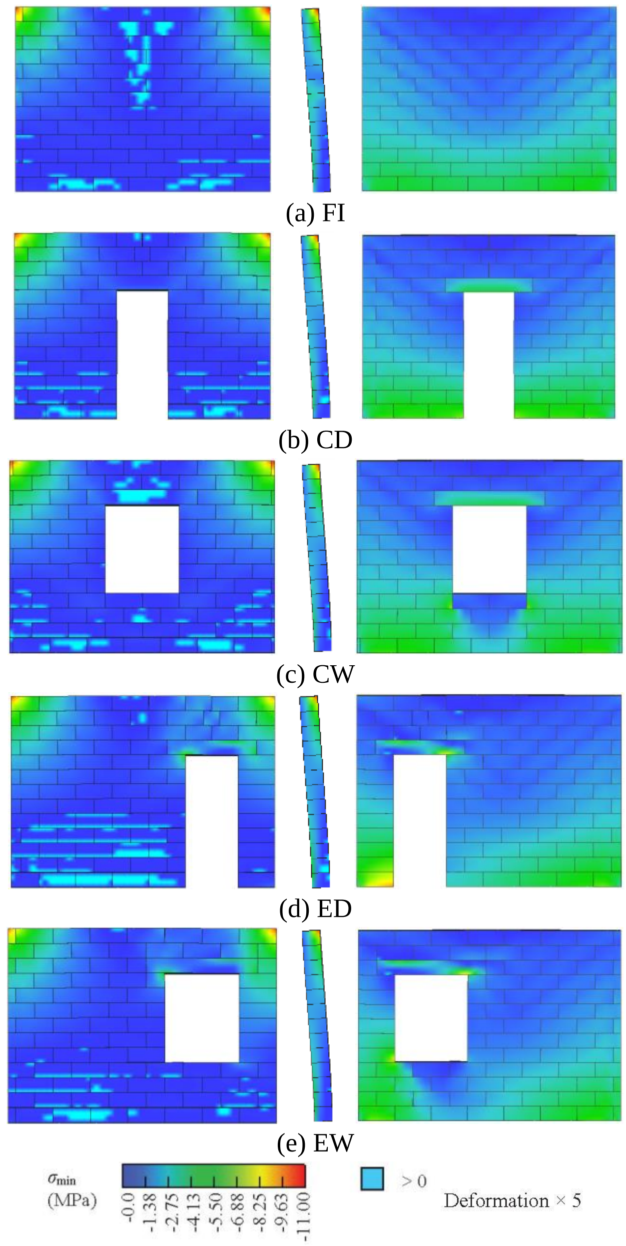

Fig. 17 Approach 2: Minimum principal stress in the infill at maximum force *W* (left front, right back view)

the frame and the infill (Figs. 16, 17).

Considering Figs. 13 and 15, one can observe that in Approach 1, there was heavy damage to the infill, while, in Approach 2, the infill was only slightly damaged; however, the frame acquired heavy damage. Fig. 13 shows that cracks, with and without openings, which form the letter "*X*" pattern. The "*X*" pattern is typical occurrence as a result of a two-way arching action. Crack patterns in the case of Approach 2 were accumulated on the frame, and on the lower back surface of the panel (Fig. 15). Similar crack patterns and findings were found in the studies by Tu *et al.* (2007), Flanagan and Bennett (1999) with two-hinged arching action.

Both approaches developed corner crushing of the infill and managed to damage the frame at clamping points (Figs. 14, 17). Both approaches developed tension around the bedjoints on the back view. Tension in Approach 1 accumulated around the panel's mid-height (Fig. 14) and, in the case of Approach 2, on the lower part of the infill (Fig. 17).

5. Conclusions

A computational study was arranged to determine the differences between out-of-plane inter-storey drift and inertial methods, and also to compared them to existing dynamical findings. The study was carried on RC frame with un-reinforced masonry infill wall 3D micromodels. The micromodel was assembled by combining calibrated bare RC frame and infill with calibrated properties of out-of-plane bending. The infill also contained window and door openings, positioned centrally and eccentrically. Inertial method models pressurized the infill while fixing the frame from translation. Contrariwise, the inter-storey drift method had a frame free from translation and loading applied to the beam-column joint.

In conclusion, the two presented approaches display highly contrasting results. Namely, the accumulation of stress and thus the damage in the case of inertial approach concerned the infill and for inter-storey drift approach, the frame. Hence, two different failure mechanisms occurred. In inertial approach, three- and four-hinged arching action was developed and failure occurred in relation to the infill. On the other hand, in the inter-storey drift approach, two-hinged arching action occurred. Nevertheless, the frame failed, not the infill. The ultimate force was significantly greater in case of the inertial approach, presumably as a result of developing arching action and different boundary conditions. In the case of inertial approach, the infill contribution to the frame was unknown as there cannot be a reference to the bare frame specimens. Further, in inter-storey drift approach, infill neither influenced initial stiffness nor the frame's response before reaching the ultimate force. The influence of infill was only observed after reaching peak load, where the full infill model had better load-bearing and deformation capacities than the bare-frame model. Unlike the bare frame model, the full in model did not fail at 2.5 % d_r. Openings in inertial approach did influence the load-bearing capacities, while arching action was able to develop. It was also noticeable that opening size composition and location influenced the behavior in the case of inertial approach. For inter-storey drift approach, openings affected the behavior after reaching peak load and did not defer from each other in terms of load-bearing capacitates, meaning they were somewhat between the full infill and bare frame models. However, they failed at the same drift ratio as the bare-frame model. Both approaches showed considerable correlation with studies of the same loading method. Additionally, inter-storey drift approach 2 showed further correlations with dynamic studies on the shaking table.

In summation, the specific outlines from this studies can be drawn:

1. Inter-storey drift methods damages the frame, while inertial methods the infill;
2. Along with the previous statement and the evidence of considerable similarities between inter-storey drift and dynamical methods, the remark that frame is irrelevant in the case of pure OoP behavior may be questionable;
3. Inertial methods produce higher resistance than the inertial methods, due to different failure mechanisms and different arching-action development. Inertial methods produced the three hinged arching action, while drift methods produced less beneficial, two-hinged action. The stated arching actions are evident through the post peak behavior, crack and stress patterns;
4. Regarding inertial methods, opening did not bypass arching action; rather they limited it (lower the response). Additionally, the lintel accumulated stress; hence, it added a point in the arching action curve. Thus, made a four-hinged arching-action;
5. In inter-storey drift methods, neither the infill nor openings affected the ultimate capacity or initial stiffness. However, they affected the post-peak behavior, i.e., the bare frame model and those with openings failed at same drift ratio (2.5% d_r) while maintaining lower resistance when compared to full infill model. Note that full infill model did not fail;
6. Contrariwise, inertial method showed that opening do affect the out-of-plane behavior, such that they lowered the response when compared to the full infill model. Also, the composition of openings affects the behavior, as it presumably alters the boundary conditions;
7. Unlike the inertial method, with inter-storey drift method the frame and infill moved as a single unit;
8. It was observed that inter-storey drift and inertial methods have very little common ground, even though they represent the behavior of same phenomena.

Acknowledgements

The research presented in this article is a part of the research project FRAmed-MAsonry composites for modelling and standardization (HRZZ-IP-2013-11-3013) supported by Croatian Science Foundation and its support is gratefully acknowledged.

References

Abrams, D.P., Angel, R. and Uzarski, J. (1996), "Out-of-plane strength of unreinforced masonry infill panels", *Earthq. Spectra*, **12**, 825-844.

Akhoundi, F., Vasconcelos, G., Lourenco, P. and Silva, L. (2016), "Out-of-plane response of masonry infilled RC frames: Effect of workmanship and opening", *16th International Brick Block Masonry Conference*, Padova, Italy.

Akhoundi, F., Vasconcelos, G., Lourenço, P.B., Palha, C. and Martins, A. (2015), "Out-of-plane behaviour of masonry infill walls", *7th International Conference Sesmiology Earthquake Engineering*, Tehran, Iran.

Al Hanoun, M.H., Abrahamczyk, L. and Schwarz, J. (2019), "Macromodeling of in-and out-of-plane behavior of unreinforced masonry infill walls", *Bull. Earthq. Eng.*, **17**(1), 519-535.

American Society of Civil Engineers (ASCE) (2000), FEMA 356 Prestandard and Commentary for the Seismic Rehabilitation of Building.

Angel, R., Abrams, D.P., Shapiro, D., Uzarski, J. and Webster, M. (1994), "Behavior of reinforced concrete frames with masonry infills", University of Illinois Engineering Experiment Station. College of Engineering, University of Illinois at Urbana-Champaign.

Anić, F., Penava, D. and Sarhosis, V. (2017), "Development of a three-dimensional computational model for the in-plane and out-of-plane analysis of masonry-infilled reinforced concrete frames", *COMPDYN 2017-Proceedings of the 6th International Conference Computational Methods in Structural Dynamics and Earthquake Engineering*, **2**, Rhodes, Greece.

Anić, F., Penava, D., Legatiuk, D., Abrahamczyk, L. and Kähler, U. (2018), "The characteristics of 2D and 3D modelling approach in calibration of reinforced concrete frames cyclic behaviour", *Proceedings of the 9th International Congress Croat. Soc. Mech*., Split, Croatia.

Anić, F., Penava, D., Varevac, D. and Sarhosis, V. (2018), "Influence of clay block masonry properties on the out-of-plane behaviour of infilled RC frames", *Teh Vjesn.* https://doi.org/10.17559/TV-20180222140915.

Asteris, P.G. and Cotsovos, D.M. (2012), "Numerical investigation of the effect of infill walls on the structural response of rc frames", *Open Constr. Build. Technol.*, **6**, 164-181.

Asteris, P.G., Cavaleri, L, Di Trapani, F. and Tsaris, A.K. (2017), "Numerical modelling of out-of-plane response of infilled frames: State of the art and future challenges for the equivalent strut macromodels", *Eng. Struct*., **132**, 110-122.

Asteris, P.G., Giannopoulos, I.P. and Chrysostomou, C.Z. (2012), "Modeling of infilled frames with openings", *Open Constr. Build. Technol. J.*, **6**, 81-91.

Booth, E. and Key, D. (2006), *Earthquake Design Practice for Buildings*, Thomas Telford, London.

British Standards Institution (2016), Methods of Test for Masonry Part 2: Determination of Flexural Strength, Bs En 1052-2.

Canadian Standards Association (1978), Masonry Design and Construction for Buildings, Mississauga, Ontario, Canada.

Cervenka Consulting (2015), ATENA for Non-Linear Finite Element Analysis of Reinforced Concrete Structures, Computer Software, Version 5.6.1.0.

Cervenka, V., Jendele, L. and Cervenka, J. (2012), *ATENA Program Documentation Part 1 Theory*, Cervenka Consulting Ltd., Prague.

Chrysostomou, C.Z. and Asteris, P.G. (2012), "On the in-plane properties and capacities of infilled frames", *Eng. Struct.*, **41**, 385-402.

Crisafulli, F.J., Carr, A.J. and Park, R. (2000), "Analytical modelling of infilled frames structures- A general review", *Bull. NZ Soc. Earthq. Eng*., **33**(1), 30-47.

Dawe, J.L. and Seah, C.K. (1989), "Out-of-plane resistance of concrete masonry infilled panels", *Can. J. Civil Eng*., **16**, 854-864.

Di Domenico, M., Ricci, P. and Verderame, G.M. (2018), "Experimental assessment of the influence of boundary conditions on the out-of-plane response of unreinforced masonry infill walls", *J. Earthq. Eng*., 1-39.

Di Trapani, F., Shing, P.B. and Cavaleri, L. (2018), "Macroelement model for in-plane and out-of-plane responses of masonry infills in frame structures", *J. Struct. Eng.*, **144**(2), 04017198.

EERI (2018), https://www.eeri.org/, Earthquake Engineering Research Institute, California, USA.

El-Dakhakhni, W.W., Elgaaly, M. and Hamid, A.A. (2003), "Three-strut model for concrete masonry-infilled steel frames", *J. Struct. Eng.*, **129**(2), 177-185.

European Committee for Standardization (2004), Eurocode 2: Design of Concrete Structures - Part 1-1: General Rules and Rules for Buildings (EN 1992-1-1:2004), European Committee for Standardization, Brussels, Belgium.

European Committee for Standardization (2004), Eurocode 8: Design of Structures for Earthquake Resistance - Part 1: General Rules, Seismic Actions and Rules for Buildings (EN 1998-1:2004), Brussels: European

European Committee for Standardization (2005), Eurocode 6: Design of Masonry Structures - Part 1-1: General rules for reinforced and unreinforced masonry structures (EN 1996-1-1:2005), Brussels, Belgium.

Fenerci, A., Binici, B., Ezzatfar, P., Canbay, E. and Ozcebe, G. (2016), "The effect of infill walls on the seismic behavior of boundary columns in RC frames", *Earthq. Struct.*, **10**(3), 539-562.

Flanagan, R.D. (1994), "Behavior of structural clay tile infilled frames", Martin Maretta Energy Systems, Report

Flanagan, R.D. and Bennett, R. (1999), "Bidirectional behavior of structural clay tile infilled frames", *J. Struct. Eng.*, **125**, 236-244.

Fowler, J.J. (1994), "Analysis of dynamic testing performed on structural clay tile infilled frames", (No. Y/EN-5310), Oak Ridge National Lab., Oak Ridge, TN, USA.

Furtado, A., Rodrigues, H. and Arêde, A. (2014), "Numerical Modeling of masonry infill walls participation in the seismic behavior of RC buildings", *Open Sees Days Port*., Porto, Portugal.

Furtado, A., Rodrigues, H., Arêde, A. and Varum, H. (2015), "Experimental characterization of the In-plane and out-of-plane behaviour of infill masonry walls", *Procedia Eng.*, **114**, 862-869.

Furtado, A., Rodrigues, H., Arêde, A. and Varum, H. (2018), "Out-of-plane behavior of masonry infilled RC frames based on the experimental tests available: A systematic review", *Constr. Build. Mater.*, **168**, 831-848.

Griffith, M.C., Vaculik, J., Lam, N.T.K., Wilson, J. and Lumantarna, E. (2007), "Cyclic testing of unreinforced masonry walls in two-way bending", *Earthq. Eng. Struct. Dyn.*, **36**, 801-821.

Hak, S., Morandi, P. and Magenes, G. (2014), "Out-of-plane experimental response of strong masonry infills", *2nd European Conference on Earthquake Engineering and Seismology*, Istanbul, Turkey.

Hallquist, Å. (1970), "Lateral loads on masonry walls", Reprint 197, Norwegian Building Research Institute, Oslo, Norway.

Henderson, R., Jones, W., Burdette, E. and Porter, M. (1993), "The effect of prior out-of-plane damage on the in-plane behavior of unreinforced masonry infilled frames", *Fourth DOE Nat. Phenom. Hazards Mitig. Conf.*, 18.

Henderson, R.C., Porter, M.L., Jones, W.D. and Burdette, E.G. (2006), "Influence of prior out-of-plane damage on the in-plane behavior of masonry infilled frames", *TMS J.*, **24**, 71-82.

Hirt, M. and Lebet, J.P. (2013), *Steel Bridges: Conceptual and Structural Design of Steel and Steel-Concrete Composite Bridges*, CRC Press.

Jäger, W., Vassilev, T., Hoffmann, J. and Schöps, P. (2008), "Unreinforced masonry basement walls - a comparison of theoretical design approaches and numerical simulations", *14th International Brick Block Masonry Conference, Sydney*, Australia.

Klingner, R.E., Rubiano, N.R., Bashandy, T.R. and Sweeney, S.C. (1996), "Evaluation and analytical verification of shaking table data from infilled frames, Part 2: Out-of-plane behavior", *Proceedings of the 7th North American Masonry Conference*, Elsevier Science Ltd., Colorado.

Lotfi, S. and Mehdi Zahrai, S. (2018), "Blast behavior of steel infill panels with various thickness and stiffener arrangement", *Struct. Eng. Mech.*, **65**(5), 587-600.

Masonry Standards Joint Committee and others (1999), "Building code requirements for masonry structures", Am. Concrete Institute, Detroit, MI, 1929081022.

Mays, G.C., Hetherington, J.G. and Rose, T.A. (1999), "Response to blast loading of concrete wall panels with openings", *J. Struct. Eng*., **125**(12), 1448-1450.

McDowell, E.L., McKee, K.E. and Sevin, E. (1956), "Arching Action Theory of Masonry Walls", *J. Struct. Div.*, **82**, 1-8.

Moghaddam, H. and Goudarzi, N. (2010), "Transverse resistance of masonry infills", *ACI Struct. J.*, **107**, 461-467.

Mohamad, G., Fonseca, F.S., Vermeltfoort, A.T., Martens, D.R.W. and Lourenco, P.B. (2010), “Strength, behavior, and failure mode of hollow concrete masonry constructed with mortars of different strengths”, *Constr. Build. Mater.*, **134**, 489-496.

Onat, O. and Gul, M. (2018), “Application of artificial neural networks to the prediction of out-of-plane response of infill walls subjected to shake table”, *Smart Struct. Syst.*, **21**(4), 521-535.

Pasca, M., Liberatorea, L. and Masiani, R. (2017), “Reliability of analytical models for the prediction of out-of-plane capacity of masonry infills”, *Struct. Eng. Mech.*, **64**(6), 765-781.

Penava, D. (2012), “Utjecaj otvora na seizmičko ponašanje armiranobetonskih okvirnih konstrukcija sa zidanim ispunom”, Ph.D. Thesis, Joisp Juraj Strossmayer, University of Osijek, Osijek, Croatia.

Penava, D. and Sigmund, V. (2018), “Out-of-plane behaviour of framed-masonry walls with opening as a result of shaking table tests”, *16th World Conf Earthq Eng 16WCEE*, 1-8.

Penava, D., Sigmund, V. and Kožar, I. (2016), “Validation of a simplified micromodel for analysis of infilled RC frames exposed to cyclic lateral loads”, *Bull. Earthq. Eng.*, **14**(10), 2779-2804.

Petrus, C., Stoian, V., Mosoarca, M. and Anastasiadis, A. (2015), “Reinforced concrete frames with masonry infills. Out of plane experimental investigatin”, *Acta Technica Napocensis: Civil Eng. Arch.*, 1-10.

Preciado, A., Ramirez-Gaytan, A., Salido-Ruiz, R.A., Caro-Becerra, J.L. and Lujan-Godinez, R. (2015), “Earthquake risk assessment methods of unreinforced masonry structures: Hazard and vulnerability”, *Earthq. Struct.*, **9**(4), 719-733.

Preti, M., Migliorati, L. and Giuriani, E. (2014), “Experimental testing of engineered masonry infill walls for post-earthquake structural damage control”, *Bull. Earthq. Eng.*, **13**(7), 2029-2049.

Ricci, P., Di Domenico, M. and Verderame, G.M. (2018), “Empirical based out-of-plane URM infill wall model accounting for the interaction with in-plane demand”, *Earthq. Eng. Struct. Dyn.*, **47**(3), 802-827.

Sepasdar, R. (2017), “Experimental investigation on the out-of-plane behaviour of concrete masonry infilled RC frames”, Ms.C Thesis, Dalhausie University.

Sigmund, V. and Penava, D. (2014), “Influence of openings, with and without confinement, on cyclic response of infilled R-C frames-An experimental study”, *J. Earthq. Eng.*, **18**(1), 113-146.

Tu, Y.H., Liu, P.M. and Lin, H.P. (2007), “Out-of-plane seismic behavior of unreinforced masonry in-filled walls”, *New Horizons Better Pract.*, 1-10.

Wang, C. (2017), “Experimental investigation on the out-of-plane behaviour of concrete masonry infilled frames”, Ms.C. Thesis, Dalhousie University.

Zovkić, J., Sigmund, V. and Guljaš, I. (2013), “Cyclic testing of a single bay reinforced concrete frames with various types of masonry infill”, *Earthq. Eng. Struct. Dyn.*, **42**(8), 1131-1149.

AT